

Semiconductor-metal nanoparticle molecules: hybrid excitons and non-linear Fano effect

Wei Zhang ¹, Alexander O. Govorov ¹ and Garnett W. Bryant ²

¹ *Department of Physics and Astronomy, Ohio University, Athens, OH 45701-2979*

² *National Institute of Standards and Technology, Gaithersburg, MD 20899-8423*

(Dated: October 9, 2018)

Modern nanotechnology opens the possibility of combining nanocrystals of various materials with very different characteristics in one superstructure. The resultant superstructure may provide new physical properties not encountered in homogeneous systems. Here we study theoretically the optical properties of hybrid molecules composed of semiconductor and metal nanoparticles. Excitons and plasmons in such a hybrid molecule become strongly coupled and demonstrate novel properties. At low incident light intensity, the exciton peak in the absorption spectrum is broadened and shifted due to incoherent and coherent interactions between metal and semiconductor nanoparticles. At high light intensity, the absorption spectrum demonstrates a surprising, strongly asymmetric shape. This shape originates from the coherent inter-nanoparticle Coulomb interaction and can be viewed as a non-linear Fano effect which is quite different from the usual linear Fano resonance.

PACS numbers: 73.21.La, 71.35.Cc, 73.90.+f

Keywords: metal-semiconductor nanostructure, plasmon-exciton interaction, hybrid exciton, nonlinear Fano effects

Modern nanoscience involves both solid-state nanostructures and bio-materials. Using bio-molecules as linkers, solid-state nanocrystals with modified surfaces can be assembled into superstructures. Building blocks of these superstructures are nanowires, semiconductor quantum dots (SQD), metal nanoparticles (MNP), proteins, etc.[1, 2]. It is important to emphasize that these building blocks are composed of different materials. Thus, if the building blocks interact, the resulting superstructure may have unique physical properties. To date, several interesting phenomena in bio-conjugated colloidal nanocrystals, such as energy transfer [2], local field enhancement [3], and thermal effects [4, 5], have been explored. In parallel with bio-assembly, self-organized growth of epitaxial SQDs has become well developed. Self-assembled SQDs have excellent optical quality and atomically-sharp optical lines [6]. Furthermore, using special growth techniques, SQDs can be arranged in 1D and 2D structures[7]. This capability for nano/bio/epitaxial assembly opens up the fabrication of complex hybrid superstructures that could exploit the discrete optical response of excitons in semiconductor nanosystems and the strong optical response of plasmons in metallic nanoparticles.

In this paper, we reveal novel unusual optical properties that arise in hybrid MNP-SQD molecules and motivate experiments to investigate these properties. Hybrid molecules have already been bio-assembled and studied at room temperature (T) by several groups [2, 3, 4]. Hybrid MNP-SQD complexes can also potentially be realized with epitaxial SQDs. First attempts to integrate MNP into a solid matrix of GaAs was done in the work [8]. In the future, such MNPs built into a crystal matrix could be combined with epitaxial SQDs to realize hybrid nanocrystal molecules. The experimental methods

to study such nanostructures include photoluminescence and absorption spectroscopies [6], and Rayleigh scattering. While the effect of energy transfer from SQD to MNPs can be observed at room T , the fine-scale coherent effects of inter-nanocrystal interaction can become accessible only at low T . For such studies, nanocrystal molecules should be deposited on surface or embedded into a polymer or solid matrix. In the current state-of-art spectroscopy of epitaxial SQDs at low T , the exciton lines may have a μeV width [6]. A combination of lithography, epitaxial growth, and bio-assembly could be used to fabricate 3D structures with desired geometry.

In this letter, we study the optical properties of hybrid structure composed of a MNP and a SQD. We explore both the linear regime (for weak external field) and the non-linear regime (for strong external field). The basic excitations in the MNP are the surface plasmons with a continuous spectrum. In SQDs, the excitations are the discrete interband excitons. In the hybrid structure there is no direct tunnelling between the MNP and the SQD. However, long-range Coulomb interaction couples the excitons and plasmons and leads to the formation of hybrid excitons and to Förster energy transfer. The effect of coupling between excitons and plasmons becomes especially strong near resonance when the exciton energy lies in the vicinity of the plasmon peak. The coupling between the continuum excitations and the discrete excitations also leads to a novel effect that we call a non-linear Fano effect. We should note that the usual Fano effect was introduced for the linear regime [9]. Here we describe a non-linear Fano effect which appears at high intensity of light when the SQD becomes strongly excited. This non-linear Fano effect comes from interference between the external field and the induced internal field in the hybrid molecule. It appears at high intensities when the degree

of coherence in the system becomes strongly increased because the Rabi frequency starts to exceed the exciton broadening.

We now consider a hybrid molecule composed of a spherical MNP of radius a and a spherical SQD with radius r in the presence of polarized external field $E = E_0 \cos(\omega t)$, where the direction of polarization is specified below. The center-to-center distance between the two nanoparticles is R (see the insert of Fig. 1). For the description of the MNP we use classical electrodynamics and the quasistatic approach. Because the hybrid structure is much smaller (i.e. tens of nanometers) than the wavelength of the incident light, we can neglect retardation effects. For the SQD we employ the density matrix formalism and the following model for a spherical SQD. Due to its symmetry, a spherical SQD has three bright excitons with optical dipoles parallel to the direction α , where α can be x, y, and z [10]. The dark exciton states are not directly involved because they are not excited in the dipole limit. However, the dark states do provide a nonradiative decay channel for the bright excitons which contributes to the exciton lifetime. Using the symmetry of the molecule and a linearly polarized internal field we can obtain the appropriate Hamiltonian [11]

$$\hat{H}_{SQD} = \sum_{i=1,2} \epsilon_i c_i^\dagger c_i - \mu E_{SQD} (c_1^\dagger c_2 + c_2^\dagger c_1), \quad (1)$$

here c_1^\dagger, c_2^\dagger are the creation operators for the vacuum ground state and α -exciton state, respectively; μ is the interband dipole matrix element, E_{SQD} is the total field felt by the SQD

$$E_{SQD} = E + \frac{s_\alpha P_{MNP}}{\epsilon_{eff1} R^3}, \quad (2)$$

with $\epsilon_{eff1} = \frac{2\epsilon_0 + \epsilon_s}{3\epsilon_0}$, ϵ_0 and ϵ_s are the dielectric constants of the background medium and SQD, respectively; E the external field, $s_\alpha = 2(-1)$ for electric field polarizations $\alpha = z(y, x)$. The z-direction corresponds to the axis of the hybrid molecule. The dipole P_{MNP} comes from the charge induced on the surface of MNP. It depends on the total electric field which is the superposition of external field and the dipole field due to the SQD,

$$P_{MNP} = \gamma a^3 (E + \frac{s_\alpha P_{SQD}}{\epsilon_{eff2} R^3}), \quad (3)$$

where $\gamma = \frac{\epsilon_m(\omega) - \epsilon_0}{2\epsilon_0 + \epsilon_m(\omega)}$, $\epsilon_{eff2} = \frac{2\epsilon_0 + \epsilon_s}{3}$, $\epsilon_m(\omega)$ is the dielectric constant of the metal. The dipole of the SQD is expressed via the off-diagonal elements of the density matrix: $P_{SQD} = \mu(\rho_{21} + \rho_{12})$ [11]. These matrix elements should be found from the master equation:

$$\frac{d\rho}{dt} = \frac{i}{\hbar} [\rho, H_{SQD}] - \Gamma\rho, \quad (4)$$

where the diagonal and off-diagonal relaxation matrix elements are $\Gamma_{12} = \Gamma_{21} = 1/T_{20}$ and $\Gamma_{22} = -\Gamma_{11} = 1/\tau_0$

[11]. Here, τ_0 includes the nonradiative decay via the dark states. We note that the above procedure treats the inter-nanoparticle interaction in the self-consistent way. To solve the coupled system, we separate the high frequency part and write ρ_{12} and ρ_{21} as $\rho_{12} = \bar{\rho}_{12} e^{i\omega t}$ and $\rho_{21} = \bar{\rho}_{21} e^{-i\omega t}$. Applying the rotating wave approximation, we obtain the equations for steady state. Let $\bar{\rho}_{21} = A + Bi$ and $\Delta = \rho_{11} - \rho_{22}$, we come to the system of nonlinear equations

$$\begin{aligned} A &= -\frac{(\Omega_I + K\Omega_R)T_2 \Delta}{1 + K^2} \\ B &= \frac{(\Omega_R - K\Omega_I)T_2 \Delta}{1 + K^2} \\ (1 - \Delta)/\tau_0 &= 4\Omega_R B - 4\Omega_I A - 4G_I(A^2 + B^2), \end{aligned} \quad (5)$$

where $K = [(\omega - \omega_0) + G_R \Delta] T_2$, $\omega_0 = (\epsilon_2 - \epsilon_1)/\hbar$, $1/T_2 = 1/T_{20} + G_I$, $G = \frac{s_\alpha^2 \gamma a^3 \mu^2}{\hbar \epsilon_{eff1} \epsilon_{eff2} R^6}$, $G_R = Re[G]$, $G_I = Im[G]$, $\Omega_{eff} = \Omega_0 [1 + s_\alpha \gamma (\frac{a}{R})^3]$, $\Omega_0 = \frac{\mu E_0}{2\hbar \epsilon_{eff1}}$, and $\Omega_R = Re[\Omega_{eff}]$, $\Omega_I = Im[\Omega_{eff}]$. Here Ω_{eff} is the Rabi frequency of the SQD renormalized due to the dipole interaction with the plasmon of the MNP.

For a weak external field, we obtain the following steady state solution in the analytical form

$$\bar{\rho}_{12} = -\frac{\Omega_{eff}}{(\omega - \omega_0 + G_R) - i(\Gamma_{12} + G_I)}. \quad (6)$$

The plasmon-exciton interaction leads to the formation of a hybrid exciton with shifted exciton frequency and decreased lifetime determined by G_R and G_I , respectively. In other words, the long-range Coulomb interaction leads to incoherent energy transfer via the Förster mechanism with energy transfer rate G_I . The exciton shift G_R shows that the interaction is partially coherent. A similar theoretical formalism for Förster transfer was successfully used to describe available experimental data [4, 10].

Energy absorption. The energy absorption rate is $Q = Q_{MNP} + Q_{SQD}$, where the rate of absorption in the MNP and SQD are $Q_{MNP} = \langle \int \mathbf{j} \mathbf{E} dV \rangle$, where \mathbf{j} is the current, $\langle \dots \rangle$ is the average over time, and $Q_{SQD} = \hbar \omega_0 \rho_{22} / \tau_0$. As an example, we consider a Au MNP with radius $a = 7.5$ nm. We use the bulk dielectric constant of Au $\epsilon_m(\omega)$ taken from [12], $\epsilon_0 = 1$, and $\epsilon_s = 6.0$. The bare exciton frequency ω_0 is chosen to be 2.5 eV, close to the surface plasmon resonance of Au MNP. Typically, the plasmon peak is very broad compared with the bare exciton peak, thus a small detuning of the frequencies should have no important effect. Both the plasmon resonant frequency and the bare exciton frequency can be tuned in a wide range of energies (from blue to red) by changing the size and composition of SQD/MNP. For the relaxation times and dipole moment, we take $\tau_0 = 0.8$ ns, $T_{20} = 0.3$ ns, and $\mu = er_0$ and $r_0 = 0.65$ nm.

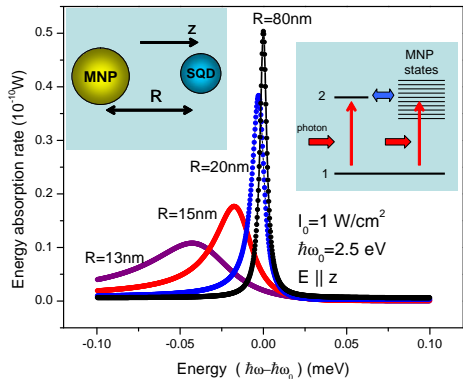


FIG. 1: Energy absorption spectra in the weak field regime for different interparticle distances. The light intensity is 1 W/cm^2 . ω is the light frequency. $\hbar\omega_0$ is the bare exciton energy. The left insert shows a model. Right insert: Quantum transitions in the system; the vertical (horizontal) arrows represent light (Coulomb)-induced transitions.

In Fig.1, we show the total energy absorption rate versus frequency. For weak incident light ($I_0 = 1 \text{ W/cm}^2$), the energy absorption peak shifts and broadens for small inter-particle separations R . This behavior of the optical spectrum for relatively small R reflects the formation of the hybrid exciton with a shifted frequency and shortened life time. In current experiments on epitaxial SQDs, the width of the exciton peak can be as small as a few μeV [6]. In our results in Fig. 1, the frequency shift is about $40 \mu\text{eV}$ for small separations $R \approx 15 \text{ nm}$.

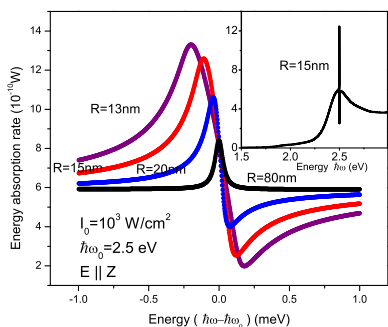


FIG. 2: Energy absorption spectra in the strong field regime for different interparticle distances. The insert is the energy absorption for $R = 15 \text{ nm}$ for a wider frequency regime; the exciton feature is within the plasmon peak.

Figure 2 shows the energy absorption in the strong field regime. We find an asymmetrical Fano shape and substantial suppression of energy absorption. This striking asymmetry originates from the Coulomb coupling and vanishes at large R (see Fig. 2).

In the usual linear Fano effect, the absorption intensity becomes zero for a particular frequency due to the

interference effect [9]. Here we find a nonvanishing energy absorption at any light frequency. This is due to the non-linear nature of the interference effect in the hybrid molecule. More qualitative discussion will be provided later. Again we see a red shift of the resonant frequency. The shift is now one order of magnitude larger than the energy resolution limit.

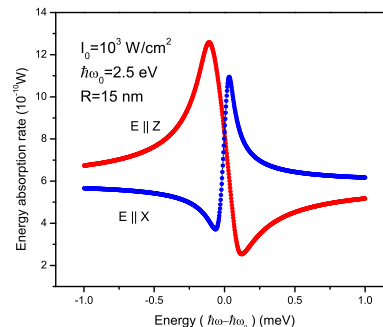


FIG. 3: Polarization dependence for the energy absorption.

In Fig. 3, we show the polarization dependence. The Fano absorption intensity has the opposite shape for the electric field polarizations along the z and $x(y)$ directions. The shape reversal due to polarization happens in a frequency window of 1 meV , and should be an observable experimental signature.

From Eqs. (3) and (5), we see that the effective field applied to MNP and SQD is the superposition of the external field and the induced internal field. The interference between external field and internal field leads to the asymmetric Fano shape. And enhancement or suppression of the effective field depends on the polarization (s changes sign for the polarizations z and $x(y)$). So, the polarization dependence is also a result of interference of the external field and induced internal field.

Rayleigh scattering. We use the standard method to calculate Rayleigh scattering intensity [13], which is valid when the size of the scattering objects is much smaller than the wavelength of incident light: $dI/d\Omega = P_0 \sin^2(\theta)$, where the angle θ is measured from the direction of the induced dipole and $P_0 = (ck^4/\hbar)(P_{SQD} + P_{MNP})^2$.

Figure 4 shows the Rayleigh scattering in the linear and nonlinear regimes. Energy absorption and Rayleigh scattering show similar features, except that the Fano resonance in the Rayleigh scattering does not reverse its shape when the polarization is changed. From the above definition of P_0 , we see that even in the absence of interaction between MNP and SQD, there is a cross term in $|P|^2$, which leads to the asymmetric shape of Rayleigh scattering in the strong field limit. The interaction between SQD and MNP leads to a shift of the peak of scattering intensity in Fig. 4 and to the polarization depen-

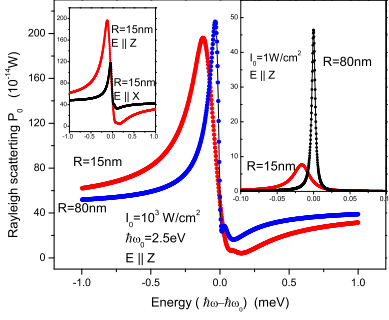


FIG. 4: Rayleigh scattering intensity P_0 . The main panel is for the strong field regime. Right insert: Scattering intensity P_0 for the weak field regime. Left insert: Intensity P_0 for different polarizations in the strong field regime.

dence (see insert of Fig. 4). In fact, the interaction effect is sensitive to polarization as we discussed before, but this dependence on the polarization may be masked by the asymmetric shape in the absence of interaction. Actually, the difference between Rayleigh scattering for the case with interaction and that for the case without interaction is sensitive to the polarization (not shown here).

As discussed above, experiments could be performed on self-assembled SQDs coupled to MNPs. The insert of Fig. 5 shows a schematic of such a system with $\varepsilon_0 = \varepsilon_s = 12$ with the MNP embedded in the barrier material that defines the SQD (here we still assume a spherical SQD for simplicity). Again we see a clear asymmetry which is strong even in the linear regime. This behavior was found for parameters typical of a self-assembled SQD. The electric field polarization was chosen along $y(x)$ directions because self-assembled lens-shape SQDs have typically two excitons with optical dipoles perpendicular to the growth direction z (insert of Fig. 5). The strong advantage of self-assembled SQDs is that an exciton in such systems exhibits a very narrow line [6].

Nonlinear Fano effect. In the linear regime, the absorption peak can have almost a Lorentzian shape (Fig. 1). Here we describe a non-linear Fano effect. This effect manifests itself as a strong asymmetry of the absorption peak at high light intensities.

The energy absorption in the weak field regime/strong field regime is

$$Q = C\Omega_0^2 \left(\frac{(K-q)^2}{1+K^2} + \alpha \frac{1}{1+K^2} \right) + \beta \frac{\hbar\omega_0}{1+K^2}. \quad (7)$$

Here $K = [(\omega - \omega_0) + G_R\Delta]T_2$, $q = \frac{s_a\mu^2\Omega_R T_2\Delta}{\hbar\varepsilon_{eff1}\varepsilon_{eff2}R^3\Omega_0}$ and the coefficient $C = \frac{1}{6} \left(\frac{2\hbar}{\mu} \right)^2 a^3 \omega \left| \frac{3\varepsilon_0}{2\varepsilon_0 + \varepsilon_m} \right|^2 \text{Im}[\varepsilon_m]$. For the weak field regime, $\alpha = \left(\frac{1}{1+G_I T_{20}} \right)^2$ and $\beta = |4\Omega_{eff}|^2 \frac{T_2^2}{T_{20}}$, and for the strong field regime $\alpha = 1$ and

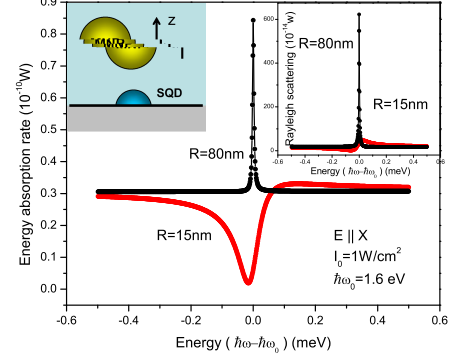


FIG. 5: Energy absorption and Rayleigh scattering (right insert) for a system with a self-assembled quantum dot in the weak field regime. The left insert: schematics of hybrid molecule. The self-assembled SQD is formed at the interface of two materials.

$$\beta = 1/2\tau_0.$$

In the weak field regime ($\Omega_0 \ll 1/T_2, 1/\tau$), Q has the Fano function form in the limit $T_{20} \rightarrow \infty$. (This was also checked by numerical calculations not shown here.) For a finite T_{20} , the finite broadening of the exciton peak may destroy the linear Fano effect and we see a symmetric peak (Fig. 1). For self-assembled SQD, the Fano asymmetry is well expressed even in the linear regime (Fig. 5). It is interesting to note that, in the regime of symmetric peak (see e.g. Fig. 1), an exciton frequency shift $\sim G_R \sim 1/R^6$. However, in the regime of nonlinear Fano effect (Fano shapes in Figs. 2,3) the resonant frequency shift $\sim 1/R^3$. Another interesting feature of the nonlinear regime is that the absorption never vanishes, even in the limit $T_{20}, \tau_0 \rightarrow \infty$.

Qualitatively, the nonlinear Fano effect can be explained as follows. When the SQD is strongly driven ($\Omega_0 \gg 1/T_2, 1/\tau$), the absorption peak becomes strongly suppressed, as in an atom [11]. For the MNP, we assume that the plasmon is not strongly excited. This is because of the very short lifetime of the plasmon (of order of 10 fs). Simultaneously, the ac dipole moments of the MNP and SQD increase with increasing intensity. In this situation, the interference between two channels of plasmon excitation in the MNP (these channels correspond to the first and second terms in the total electric field in Eq. 3) increases and the peak asymmetry is greatly enhanced. For example, the depth of the minimum in the absorption curve becomes comparable to the peak height in Fig. 2.

It is possible to show that the problem of Förster-like interaction between SQD and MNP is equivalent to the Fano problem [9]. To solve this problem, we can also use the density matrix formulation for a description of the plasmon excitations in MNP and look at the interaction between continuum plasmon states and discrete exciton states directly, without employing a self-consistent ap-

proach. Then by using the fluctuation-dissipation theory [10, 14], we are able to recover the previous results in the linear regime with fast relaxation in MNP.

In conclusion, we have studied the optical properties of a hybrid nanostructure composed of a MNP and a SQD. The interaction between plasmon and exciton leads to interesting effects such as Förster energy transfer, exciton energy shift, and interference. The energy absorption and Rayleigh scattering reveal the formation of collective hybrid excitons. At high light intensity, we find a novel nonlinear Fano resonance which has striking differences to the usual Fano effect.

Acknowledgments We acknowledge helpful discussions with Dr. T. Klar in Physics Department and CeNS, Ludwig-Maximilians-Universität München, Germany. This work was supported by NIST and BioTechnology Initiative at Ohio University.

-
- [1] Y. Cui, et al, Science 293, 1289 (2001); Y. A. Yadong, et al, Nature 437, 664 2005; E. Dulkeith et al., Nano Lett. 5, 585 (2005).
 - [2] J. Lee et al., Nano Lett. 4, 2323 (2004).
 - [3] K. T. Shimizu et al., Phys. Rev. Lett. 89, 117401 (2002).
 - [4] J. Lee et al., Angew. Chem. 117, 7605 (2005); K. T. Slock et al., Supramol. Chem., (2006), in press.
 - [5] H. Richardson et al., Nano Lett. 6, 783 (2006).
 - [6] J. R. Guest et al., Phys. Rev. B 65, 241310(R) (2002); A. Högele et al., Phys. Rev. Lett. 93, 217401 (2004); H. Htoon et al., Phys. Rev. Lett., 88, 087401 (2002).
 - [7] Zh. M. Wang et al., Appl. Phys. Lett. 86, 143106 (2005).
 - [8] D. C. Driscoll et al., Appl. Phys. Lett. 86, 051908 (2005).
 - [9] U. Fano, Phys. Rev. 124, 1866 (1961).
 - [10] A. O. Govorov et al., Nano Lett. (2006), DOI:10.1021/nl060105l.
 - [11] A. Yariv, Quantum Electronics, New York, John Wiley and Sons, 1975.
 - [12] E. D. Palik, Handbook of Optical Constant of Solids, New York, Academic Press, 1985.
 - [13] J. D. Jackson, Classical electrodynamics, 2nd ed. New York : Wiley, 1975.
 - [14] P. M. Platzman, Waves and Interactions in Solid State Plasmas, New York, Academic Press, 1973.

[1] Y. Cui, et al, Science 293, 1289 (2001); Y. A. Yadong, et al, Nature 437, 664 2005; E. Dulkeith et al., Nano Lett.